ELSEVIER

S0032-3861(96)00220-0

Polymer Vol. 37 No. 17, pp. 3851–3860, 1996

0032-3861/96/$15.00 + 0.00

Solubility and dynamic mechanical behaviour of polyurethane systems at the critical molar ratio of the reactive groups for gelation and at the gel point

M. Ilavský*, Z. Bubeníková and K. Bouchal
Institute of Macromolecular Chemistry, Academy of Sciences of the Czech Republic, 162 06 Prague 6, Czech Republic

and J. Fähnrich
Faculty of Mathematics and Physics, Charles University, 180 00 Prague 8, Czech Republic
(Received 17 March 1995; revised 31 October 1995)

The dynamic mechanical behaviour of fully cured soluble and insoluble polyurethanes from two poly(oxypropylene)triols and a diisocyanate with initial ratios $r_H = [OH]/[NCO]$ from 1.44 to 1.8 were investigated. The dynamic behaviour during the curing reactions of two samples with $r_H = 1$ was also measured. From extraction experiments the critical ratios for gelation r_H^c of fully cured samples were determined. As expected, both critical gel (CG) samples in which the gel point was reached by changing the conversion exhibit a power-law rheological behaviour. On the other hand, both fully cured CG samples prepared at r_H^c show a small frequency dependence of the loss tangent so that critical power-law behaviour is not exactly obeyed. New conditions representing critical rheological behaviour are suggested. Copyright © 1996 Elsevier Science Ltd.

(Keywords: dynamic mechanical behaviour; polyurethanes; gel point)

INTRODUCTION

A polymerization with at least one of the reactants having a functionality greater than two is characterized by disproportionate increases in the number-average and weight-average molecular weights, M_n and M_w. At the critical conversion (the gel point, GP), M_w and the steady-state shear viscosity of the system increase to infinity. In the pre-gel state the system is soluble (liquid-like structure) and after passing the GP the insoluble gel fraction, w_g, characterized by a finite equilibrium modulus, G_e, is formed in the reacting system (solid-like structure). The material at the GP, termed the critical gel (CG), is in an intermediate state between solid and liquid.

Classical GP determination is based on solubility experiments. However, in recent years it has been demonstrated that the GP can be also determined from dynamic mechanical measurements. After the first proposal[1] that the GP is given by the crossover of the dynamic storage (G') and loss (G'') shear moduli (loss tangent $\tan\delta = G''/G' = 1$, $G'' > G'$ for the pre-gel and $G'' < G'$ for the post-gel state should be valid), further experiments have revealed that the CG is characterized by a power-law static shear relaxation modulus $G(t)$[2–4]

$$G(t) = St^{-n} \tag{1}$$

where t is the time, S (Pa s^n) is the gel strength ($S = G_0\tau_0^n$, where the modulus G_0 and relaxation time τ_0 are specific material parameters[4]) and n is a critical exponent. From equation (1), using the Fourier transform, it follows for the storage and loss dynamic shear moduli at the GP

$$G'(\omega) = G''(\omega)/\tan\delta = \Gamma(1-n)\cos\delta\, S\omega^n \tag{2}$$

where $\Gamma(x)$ is the gamma function and the phase angle $\delta = n\pi/2$ is independent of frequency. Equation (2) shows that a power-law behaviour is also found in the dynamic experiments. The power-law behaviour is the consequence of structural self-similarity which evolves during network formation at length scales from chain up to sample dimensions. The exponent n appeared to be sensitive to the composition of a reacting system and to the type of reaction, and values of n from 0.2 to 0.9 can be found in the literature[2–6].

In polyurethane systems prepared from polyisocyanates and polyols by the reaction of isocyanate (NCO) and hydroxyl (OH) groups (as well as in other end-linked systems) there are two ways of reaching the GP. Both ways follow from the well known GP equation[7–10] valid for independent reactivities of OH and NCO groups in the reactive oligomers

$$\alpha_H^c\alpha_I^c(f_{w,H}-1)(f_{w,I}-1) = 1 \tag{3}$$

where α_H^c and α_I^c are the critical (gel point) conversions of hydroxy and isocyanate groups, and $f_{w,H}$ and $f_{w,I}$ are the weight-average functionalities of polyol and

* To whom correspondence should be addressed

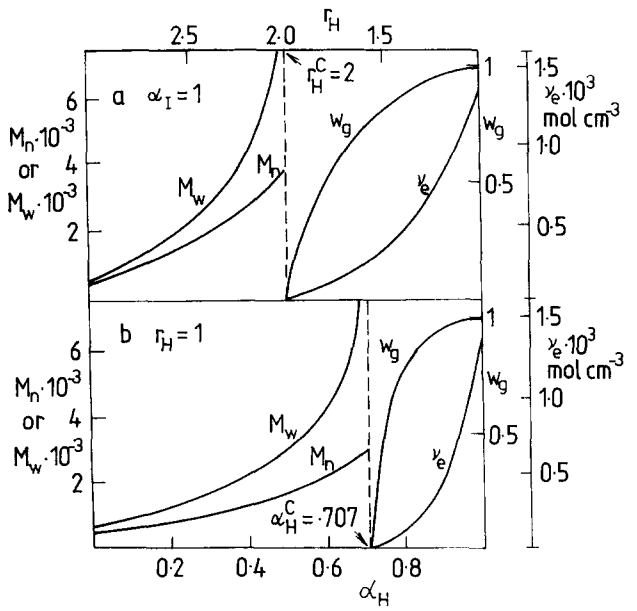

Figure 1 Schematic changes in structural parameters during network formation in a monodisperse triol ($f_{n,H} \equiv f_{w,H} = 3$, $M_{n,H} \equiv M_{w,H} = 750$) with monodisperse diisocyanate ($f_{n,I} \equiv f_{w,I} = 2$, $M_{n,I} \equiv M_{w,I} = 250$) system[14]. M_n and M_w are, respectively, the number- and weight-average molecular weights, ν_e is concentration of elastically active network chains, α_H and α_I are conversions of hydroxyl and isocyanate groups, respectively, w_g is the weight fraction of the gel and r_H is initial ratio of reactive groups. For calculation of molecular weights M_n and M_w, equations (17) and (18) were used. The ν_e and w_g values were calculated from equations (A-20) and (A-15) of ref. 12. (a) Evolution of network structure with the change in the reactive group ratio for full conversions of minority (isocyanate) groups, $\alpha_I = 1$. At the initial molar ratio $r_H = 3$ the molecular weights of the system are $M_N = 583$ and $M_w = 680$, and at the critical molar ratio $r_H^c = 2$ (the gel point) the values are $M_n = 3758$ and $M_w \to \infty$; the molecular weight of the elastically active network chains, $M_e = (2/3) \times M_{n,H} + M_{n,I} = 750$, which gives $\nu_e = 1.33 \times 10^{-3}$ mol cm^{-3} (considering the network density $\rho = 1$ g cm^{-3}). (b) Evolution of network structure with conversion for stoichiometric ratio $r_H = 1$. In the initial stage of reaction $\alpha_H = 0$, the molecular weights are $M_n = 450$ and $M_w = 583$, and at the gel point, $\alpha_H^c = 0.707$, $M_n = 2970$ and $M_w \to \infty$; the value $\nu_e = 1.33 \times 10^{-3}$ mol cm^{-3} is the same as in case (a). (- - - -) Gel point conditions

polyisocyanate, respectively. The reduced second moments of the functionality distributions $f_{w,H}$ and $f_{w,I}$ are given by

$$f_{w,H} = \sum i^2 n_H^i / \sum i n_H^i = \sum i^2 n_H^i / f_{n,H}$$
$$f_{w,I} = \sum j^2 n_I^j / \sum j n_I^j = \sum j^2 n_I^j / f_{n,I} \quad (4)$$

where n_I^j and n_H^i are the mole fractions of the j-functional polyisocyanate component and the i-functional polyol component, respectively ($\Sigma n_H^i = \Sigma n_I^j = 1$). $f_{n,I}$ and $f_{n,H}$ are the number-average functionalities (the first moments of the functionality distributions) of polyisocyanate and polyol, respectively. If the reaction of NCO and OH groups is carried out at an off-stoichiometric ratio of the reactive groups then the relation

$$\alpha_B r_H = \alpha_I \quad (5)$$

is valid between the conversion of [OH] and [NCO] groups. The initial molar ratio of hydroxyl to isocyanate groups $r_H = [OH]/[NCO]$.

The increase in conversion at constant composition of a reacting system ($r_H = $ const.) represents the first, classical way of reaching the CG at critical conversion α_H^c. From equation (3) we have

$$\alpha_H^c = [r_H(f_{w,H} - 1)(f_{w,I} - 1)]^{-1/2} \quad (6)$$

For conversions $\alpha_H < \alpha_H^c$, the system is soluble and for $\alpha_H > \alpha_H^c$ the reacting system contains both insoluble gel and soluble sol fractions. CG properties are usually determined during the reaction without stopping it although an attempt to stop the reaction close to the GP by quenching the sample was also made[2]. Schematic changes of the structural parameters, molecular weights M_n, M_w, gel fraction w_g and concentration of elastic chains ν_e with α_H are shown in *Figure 1b* for the reaction of monodisperse triol ($f_{n,H} \equiv f_{w,H} = 3$, $M_{n,H} \equiv M_{w,H} = 750$) with monodisperse diisocyanate ($f_{n,I} \equiv f_{w,I} = 2$, $M_{n,I} \equiv M_{w,I} = 250$) at $r_H = 1$.

The second way of reaching the CG is the critical molar ratio (CMR) method, consisting of finding the critical initial ratio of the reactive groups r_H^c (i.e. finding critical composition) at which the GP occurs just when the conversion of minority groups approaches 100%[9–11]. From equations (3) and (5), for the case $r_H > 1$ ($\alpha_H^c \times r_H^c = \alpha_I^c$), the CG structure is reached at the critical molar ratio of r_H^c given by

$$r_H^c = (\alpha_I^c)^2 (f_{w,H} - 1)(f_{w,I} - 1) \quad (7)$$

In this case the samples with ratios $r_H > r_H^c$ are soluble and the systems with $r_H < r_H^c$ contain both sol and gel. The change in the structural parameters, M_n, M_w, w_g and ν_e with r_H is shown in *Figure 1a* for reaction of diisocyanate with triol and full conversion of minority (NCO) groups ($\alpha_I = 1$). While the change in the conversion at constant composition (constant r_H) leads to reacting structures, the change in the reactive groups ratio at full conversion of minority groups gives structurally stable samples. Although one dynamic mechanical measurement of a polyurethane sample prepared close to r_H^c has been made previously[6], the systematic solubility and dynamic mechanical studies of CG structures prepared by the CMR method have not been made so far.

In this work we have studied the extraction and dynamic mechanical behaviour of polyurethane systems based on two poly(oxypropylene)triols and 4,4′-diphenylmethane diisocyanate in the vicinity of the CG reached by the CMR method. As non-reactive stable samples prepared with an excess of hydroxyl groups to the full conversion of the isocyanate groups are used, the mechanical measurements were carried out over broad frequency and temperature intervals, from glassy to rubbery (or flow) regions. For comparison, an evolution of the dynamic behaviour with reaction time during curing at constant temperature for the stoichiometric ratio of reactive groups $r_H = 1$ was also studied.

EXPERIMENTAL

Materials and characterization

Two poly(oxypropylene)-triols (PPT, Union Carbide Niax Polyols) were dried by azeotropic distillation with benzene to remove water (the remaining residual water determined by coulometry was less than 0.2 wt% in both cases). The number-average molecular weights,

M_n, determined by v.p.o. were 710 (LHT-240) and 2630 (LG-56). The concentration of hydroxyl groups was determined by reaction with an excess of phenyl isocyanate (PI); the unreacted PI was reacted with dibutylamine and its excess was determined by potentiometric titration with HCl. The OH contents in LHT-240 and in LG-56 were 6.94 and 1.8 wt%, respectively, giving number average functionalities, $f_{n,H} = 2.89$ (LHT-240) and 2.78 (LG-56). As was shown earlier[12], both triols were composed of bi- and trifunctional components with mole fractions $n_H^2 = 0.11$ and $n_H^3 = 0.89$ (LHT-240), and 0.22 and 0.78 (LG-56), respectively. Using these mole fractions, the weight average functionalities [equation (4)] $f_{w,H}$ are 2.92 (LHT-240) and 2.84 (LG-56), respectively.

4,4′-Diphenylmethane diisocyanate (MDI) was distilled under reduced pressure and then recrystallized twice from dry hexane. The solvent was removed under oil pump vacuum at room temperature. The purity of MDI determined by titration was 99.5% ($f_{n,I} = f_{w,I} = 2$, $M_n = 250$).

Sample preparation

PPT mixed with MDI was stirred for ~15 min in a closed glass vessel in a dry nitrogen atmosphere at 55–60°C and 0.005 wt% of dibutyltin dilaurate was then added. After that, the mixture was dosed into closed Teflon moulds. The polymerization proceeded for 48 h at 80°C and after that the temperature was decreased to 25°C. Spectroscopic measurements revealed that no NCO groups were present at the end of the reaction. With each PPT a series of samples was prepared with variable initial compositions characterized by the molar ratio of OH and NCO groups, $r_H = [OH]/[NCO]$ ranging from 1.44 to 1.80. Before rheological measurements, moulds were cooled down to −50°C, and sheets ($10 \times 10 \times 0.2\,cm^3$) were removed; samples 50, 30 and 10 mm in diameter were cut from the sheets and used in parallel-plate-geometry mechanical measurements.

Two samples prepared at the stoichiometric ratio of reactive groups, $r_H = 1$, were used to study the evolution of dynamic behaviour during curing. A mixture of PPT and MDI was homogenized at 55–60°C as in the preceding cases and then quickly transferred onto the preheated plates of the rheometer. The cure temperature was 60°C for samples of both PPT's.

Dynamic mechanical measurements and extraction

Dynamic mechanical behaviour was measured with a Rheometrics SYS-4 apparatus. Small-strain oscillatory shear measurements were performed with parallel-plate geometry. Strains between $\gamma = 0.2$ and 0.001 were employed (linear viscoelasticity). The angular rate ω varied from 10^{-2} to $10^2\,rad\,s^{-1}$ and the temperature interval was from −50 to 100°C. While at the beginning of the main transition and glassy regions plates 10 mm in diameter were used, at the end of the transition and in rubbery or flow regions, 30 and 50 mm diameters were used. During measurement at constant temperature strain was decreased with increasing frequency. The real, G', and imaginary, G'', components of the complex shear modulus, the real, J', and imaginary, J'', components of complex shear compliance and loss tangent, $\tan\delta\,(= J''/J' = G''/G')$ were determined.

By applying the frequency–temperature superposition to the experimental data, superimposed curves of mechanical functions (e.g. $G'_p = G'b_T$ or $J''_p = J''/b_T$, etc., vs reduced frequency ωa_T) shifted to the reference temperature $T_0 = 30$°C were obtained for all samples of both series. The horizontal shift factor a_T was obtained mainly from the superposition of loss tangent (since for tan δ no vertical shift is necessary, $\tan\delta_p = \tan\delta$), while the vertical shift factor b_T was obtained from the superposition of G' and G''.

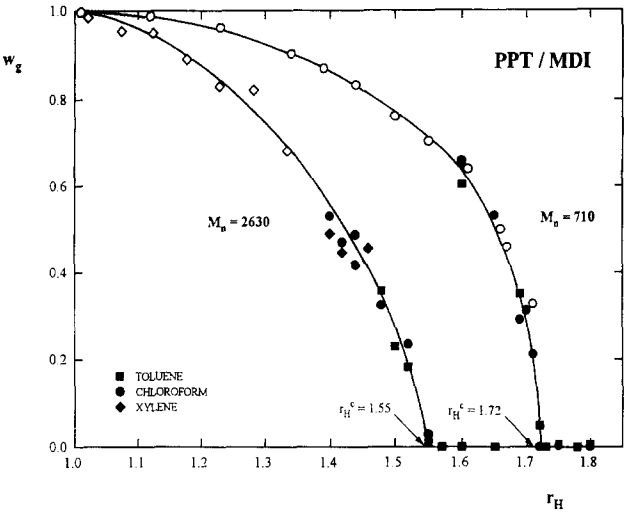

Figure 2 Dependence of the weight fraction of gel, w_g, on the ratio of reactive groups r_H. r_H^c are the critical ratios for gelation. ○, ◇ Data obtained earlier[12]

The curing reaction was followed in rheometer at various frequencies ($1-100\,rad\,s^{-1}$), with parallel plate geometry (diameter 50 mm) at the curing temperature $T_c = 60$°C. The shear strain was reduced during curing from $\gamma = 1$ to 0.005 to avoid network breakdown (near the GP, the values $\gamma = 0.1-0.01$ were used). A series of frequency sweeps (one run takes 60 s) during curing was obtained.

The extraction of the samples was carried out with a large excess of xylene, toluene or chloroform at room temperature for several weeks. The samples were placed inside a Teflon mesh (sieve) and immersed in the solvent. After extraction, the mesh with an extracted sample was dried under reduced pressure at 60°C and the weight fraction of the gel, w_g, was determined from the weight of the sample before and after the extraction.

RESULTS AND DISCUSSION

Extraction, critical molar ratio of reactive groups r_H^c and concentration of elastically active network chains

The weight fraction of gel, w_g, as a function of the reactive group ratio, r_H, in both series of networks is given in *Figure 2* in which the data[12] published earlier are also included. The expected decreased in w_g with increasing deviation from stoichiometry for networks of both polyols was found and the values of the critical molar ratio of reactive groups, r_H^c, could be determined ($r_H^c = 1.72$ for LHT-240 and $r_H^c = 1.55$ for LG-56). While samples with $r_H^c > r_H^c$ are soluble, those with $r_H < r_H^c$ are networks. The r_H^c values found for samples from LG-56 are lower than those for samples from LHT-240 due to a lower functionality of the long triol in comparison with the short triol [see equation (7)].

The published theory[12] of network formation, based

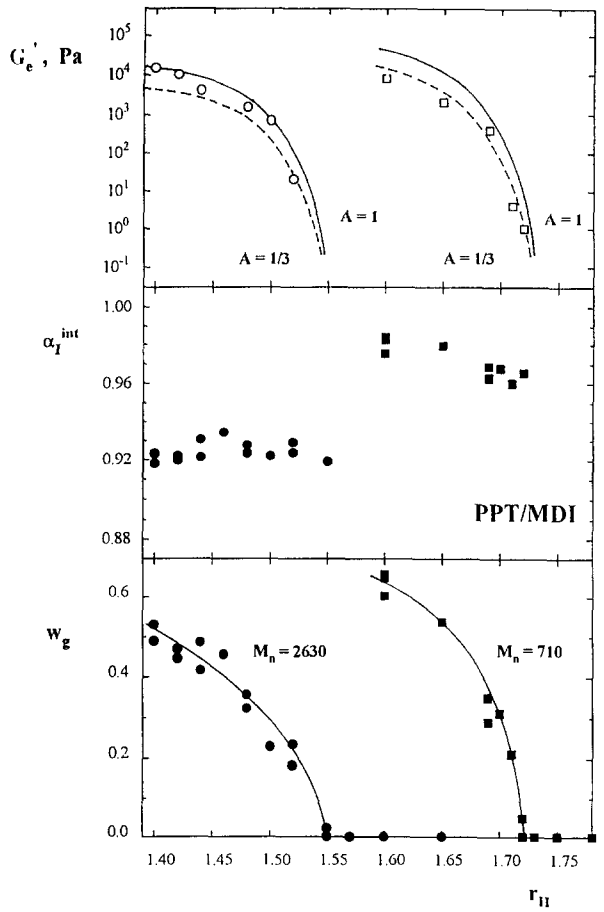

Figure 3 Dependence of the weight fraction of the gel, w_g, the intermolecular conversion of the isocyanate groups, α_I^{int}, and the extrapolated equilibrium values of the storage modulus, G_e', on the ratio of the reactive groups r_H. Average theoretical dependences (equation 8) for: (——) $A = 1$, (- - -) $A = 1/3$

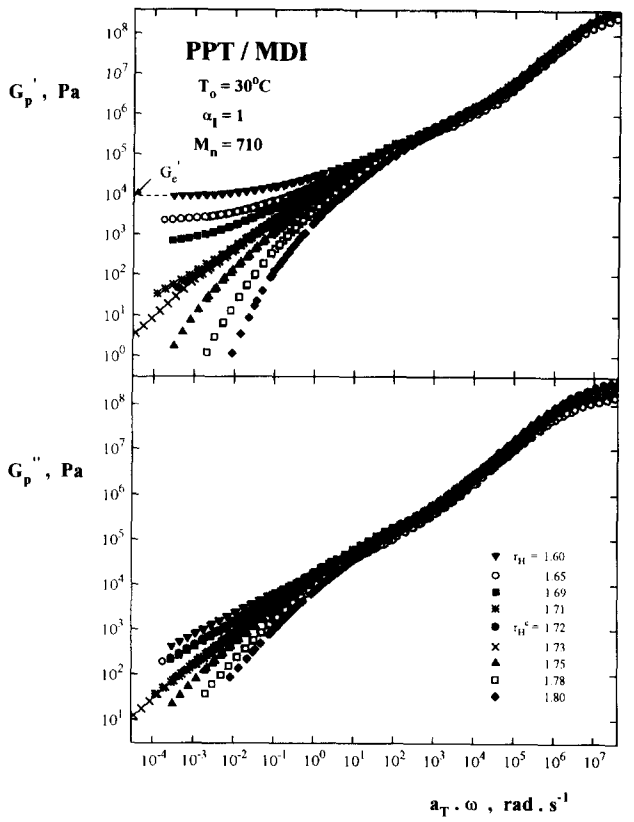

Figure 4 Dependence of the reduced storage and loss moduli, G_p' and G_p'', on the reduced frequency, ωa_T, for $T_0 = 30°C$ and triol LHT-240 for samples prepared at indicated r_H values

on the theory of branching processes, in which only the formation of urethane groups without cyclization is considered, has been used to describe the experimental dependences of w_g on r_H. In calculations, we suppose that PPT's are composed of di- and trifunctional components with same M_n (see Materials). Using equation (A-15) from ref. 12 it is possible to calculate, from experimental w_g values, the apparent intermolecular conversions of NCO (minority) groups, α_I^{int}, which correspond to the ring-free case. From the w_g values of our samples, the calculated conversions are $\alpha_I^{int} = 0.96–0.98$ for LHT-240 and 0.92–0.94 for LG-56 (*Figure 3*); similar α_I^{int} values were found earlier[12] for the same networks prepared with lower r_H ratios. As calculated earlier[12], an approximate fraction of bonds wasted in cycles varied by about 3–4%, and if these values are added to α_I^{int} the total conversions of $\alpha_I \sim 1$ for networks from LHT-240 and $\alpha_I \sim 0.96–0.98$ for networks from LG-56 may be expected. It was proved earlier[12–14] that no side reactions take place in the region of excess of hydroxyl groups.

As follows from equation (7), the experimental r_H^c values are considerably lower than would correspond to a ring-free case [if $\alpha_I^c = 1$, then r_H^c values should be 1.92 (LHT-240) and 1.84 (LG-56), respectively]. The apparent conversions α_I^c calculated from r_H^c are 0.96 (LHT-240) and 0.94 (LG-56). It can be seen from *Figure 3* that α_I^c are similar to α_I^{int} values calculated from gel fractions w_g.

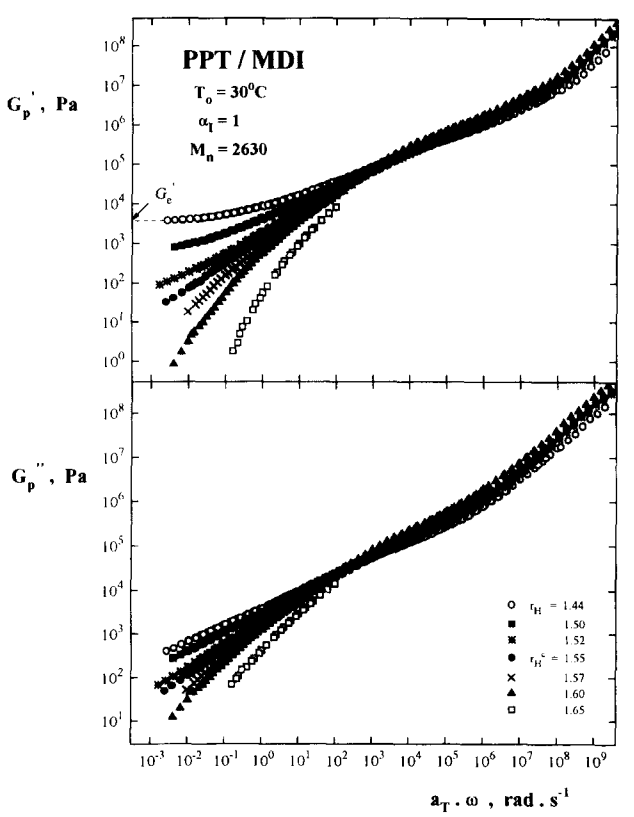

Figure 5 Dependence of the reduced storage and loss moduli, G_p' and G_p'', on the reduced frequency, ωa_T, for $T_0 = 30°C$ and triol LG-56 for samples prepared at indicated r_H values

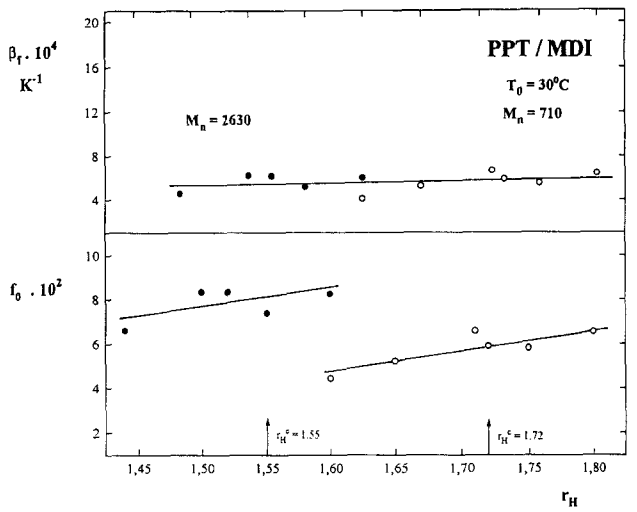

Figure 6 Dependence of the fractional free volume, f_0, and of the free volume temperature expansion coefficient, β_f, on the ratio r_H. r_H^c are the critical ratios for gelation

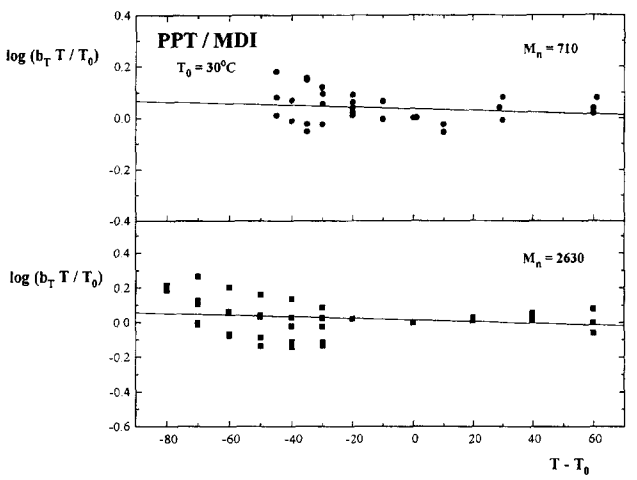

Figure 7 Temperature dependence of the reduced vertical shift factor $b_T T/T_0$

From frequency dependences of the superimposed storage modulus G'_p deep in the rubbery region (at the lowest ωa_T), the extrapolated equilibrium values G'_e were obtained (see *Figures 4* and *5*) for networks of both polyols prepared with $r_H < r_H^c$. Assuming that the sol and gel have the same density and that the sol acts as a diluent, the value of modulus G'_e is given by[10]

$$G'_e = A\nu_c w_g RT_x \tag{8}$$

where R is the gas constant, $T_x = 303\,K$, ν_c is the chemical concentration of elastically active network chains (EANC) and A is the front factor[15] ($A = 1$ for affine and $A = 1/3$ for phantom networks). The ν_c values were calculated for both series using apparent conversions α_I^{int} from equation (A-20) of ref. 12. *Figure 3* shows a comparison between the experimental G'_e values and those theoretically predicted for the front factor $A = 1$ and $A = 1/3$. It can be seen that the experimental data are placed within both limits. While the data of LHT-networks are close to $A = 1/3$, those of LG-networks are above the $A = 1/3$ limit; similar behaviour was observed earlier[12,13].

It can be concluded that branching theory, in which the functionality distribution of PPT's is accounted for, describes to a first approximation the dependence of w_g and G'_e on r_H if apparent intermolecular conversions are used.

Dynamic mechanical behaviour

Stable systems prepared at various r_H ratios. Temperature dependences. For all samples of both series the frequency–temperature superposition could be performed and the temperature dependences of the horizontal shift factors satisfied the Williams–Landel–Ferry (WLF) equation in the form

$$\log a_T(T_0) = -(1/2.3f_0)(T - T_0)/(f_0/\beta_f + T - T_0) \tag{9}$$

where f_0 is the fractional free volume at reference temperature $T_0 = 30°C$ and β_f is the thermal expansion coefficient of the free volume. From *Figure 6* it can be seen that the free volume parameters are only slightly dependent on the composition of the samples. While the coefficient $\beta_f \doteq 5 \times 10^{-4}\,K^{-1}$ is close to the universal value ($= 4.8 \times 10^{-4}\,K^{-1}$)[16] and roughly independent of M_n of triols and of the ratio r_H, the free volume f_0 is larger for the long triol ($f_0 \doteq 0.08$) than for the short triol ($f_0 \doteq 0.06$). This is due to the fact that the main transition region of samples from LG-56 is located at lower temperatures and higher frequencies than that of samples prepared from LHT-240. As no abrupt changes in dependences of the free-volume parameters on r_H can be found at critical ratios r_H^c, the GP has no specific effect on the temperature dependence of the relaxation times.

The temperature dependences of reduced vertical shift factors, $\log(b_T T/T_0)$, of both series are shown in *Figure 7*. While the Rouse–Mooney theory of viscoelastic behaviour led to prediction[16]

$$b_T(T_0) = (T\rho)_{T_0}/(T\rho)_T \tag{10}$$

where ρ is the density, modification of this theory for permanent networks gave[17]

$$b_T(T_0) = (\rho^{1/3T}/\langle r_0^2\rangle)_{T_0}/(\rho^{1/3}T/\langle r_0^2\rangle)_T \tag{11}$$

in which $\langle r_0^2\rangle$ is the mean square end-to-end distance of the network chain in the reference state ($\langle r_0^2\rangle$ can contribute to the temperature dependence of b_T due to a change in the population of rotational isomers with temperature). Despite the large scatter of data in *Figure 7*, if we suppose that the dependences of $\log(b_T T/T_0)$ on $T - T_0$ are linear, small negative slopes $s = -4 \times 10^{-4}\,K^{-1}$ (LHT-240) and $-5 \times 10^{-4}\,K^{-1}$ (LG-56) were found. Similar behaviour was observed earlier for other systems[18].

Frequency dependences. The dependences of superimposed curves of the storage and loss moduli, G'_p and G''_p, and of the loss tangent, tan δ_p, on the reduced frequency ωa_T at reference temperature $T_0 = 30°C$ for both series are shown in *Figures 4*, *5* and *8*. The shape and position of the main transition region (located at high frequencies) on the frequency are only slightly dependent on the ratio r_H. As expected, the frequency of the tan δ_p maximum, ω_m, of samples prepared from LG-56 is three orders of magnitude higher than that of

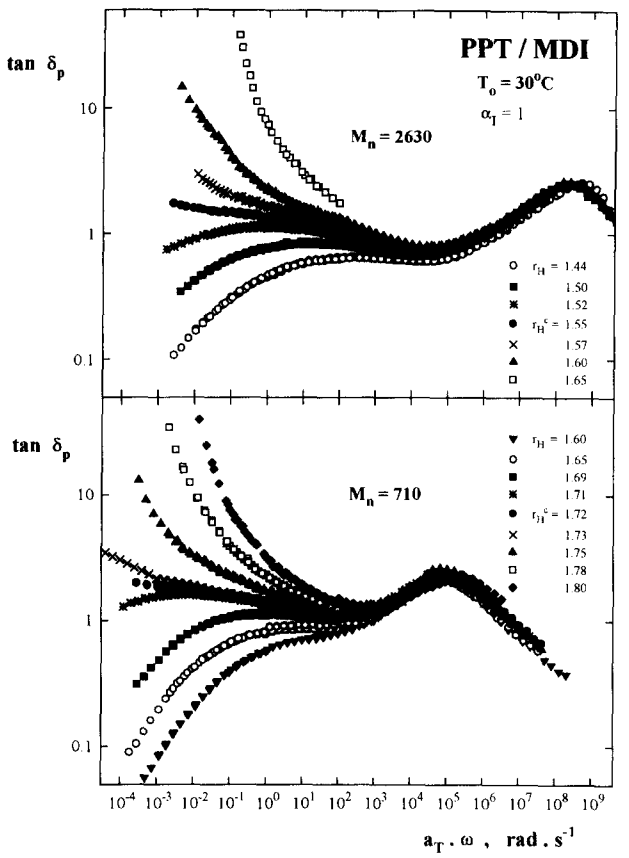

Figure 8 Dependence of the reduced loss tangent, tan δ_p, on the frequency, ωa_T, for $T_0 = 30°C$ for samples prepared at indicated r_H values

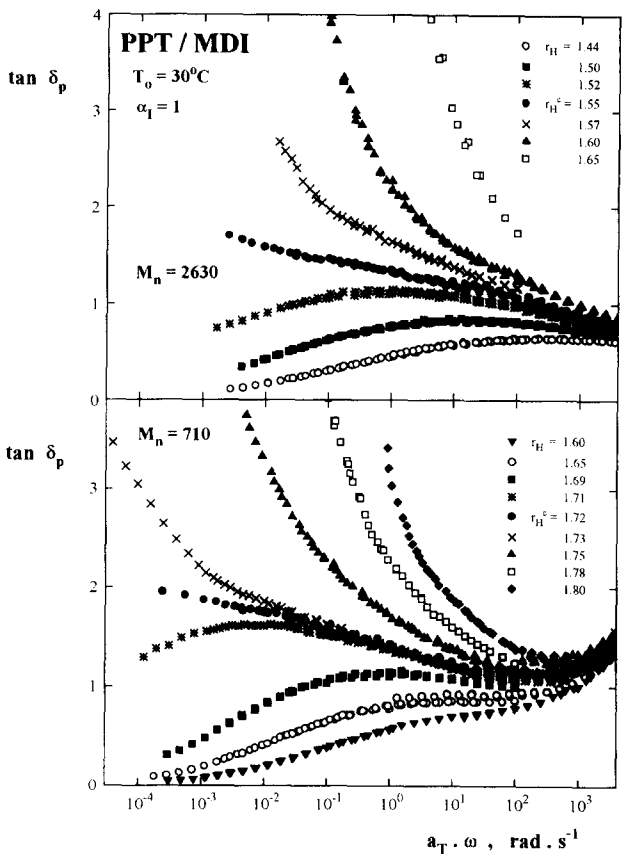

Figure 10 Dependence of the reduced loss tangent, tan δ_p, on the frequency, ωa_T, for $T_0 = 30°C$ in the rubbery and flow regions for samples prepared at indicated r_H values

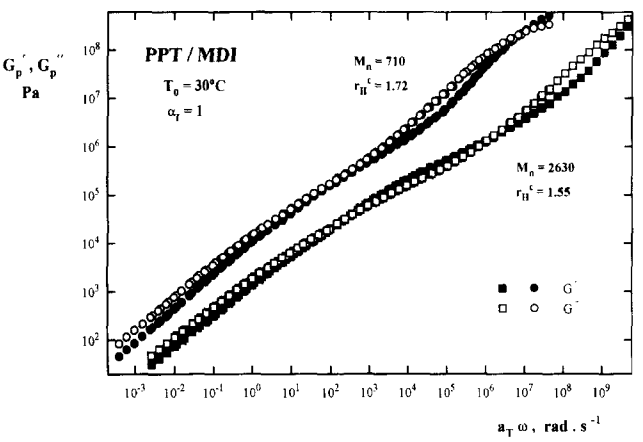

Figure 9 Frequency dependence of the reduced storage and loss moduli, G'_p and G''_p, for CG samples prepared at $r_H^c = 1.72$ (LHT-240) and $r_H^c = 1.55$ (LG-56)

samples prepared from LHT-240 [$\omega_m \sim 10^8$ (LG-56) and $\omega_m \sim 10^5$ rad s^{-1} (LHT-240)]. On the other hand, a large change in the shape of the frequency dependences of the dynamic functions, especially of the superimposed loss tangent, tan δ_p, in the rubbery and flow regions with the ratio r_H can be seen. While for all network samples ($r_H < r_H^c$) tan δ_p decreases with decreasing reduced frequency ωa_T (solid-like behaviour), for soluble samples ($r_H > r_H^c$) tan δ_p increases with decreasing ωa_T (liquid-like behaviour). At the same time, in network samples non-zero values of equilibrium storage modulus G'_e can be found by extrapolation. At constant frequency ωa_T, the values of the modulus G'_p decrease and tan δ_p increase with increasing ratio r_H for both series of samples.

For both samples with the critical gel structure prepared at r_H^c, the linear dependences of log G'_p and log G''_p on log ωa_T can be seen in the low-frequency region [$\omega a_T < 10^1$ (LHT-240) and $<10^2$ (LG-56) rad s^{-1}] where power-law behaviour should be observed (*Figure 9*). Surprisingly, the slopes s_1 found for storage modulus ($s_1 = 0.70$ and 0.63 for LTH-240 and LG-56, respectively) differ from those s_2 found for the loss modulus ($s_2 = 0.66$ and 0.59 for LTH-240 and LG-56, respectively). Due to this fact, the loss tangent, tan δ_p, is slightly dependent on frequency for both critical gel samples. From *Figure 10* which illustrates this behaviour in detail, one can mention that not only critical samples with r_H^c but also two others with the closest r_H ratios ($r_H = 1.71$ and 1.73 for LHT-240 and $r_H = 1.52$ and 1.57 for LG-56) show a region (after the transition) with the same increase in tan δ_p with decreasing ωa_T (especially for triol with $M_n = 710$) as critical samples.

In the first approximation, we can write for both critical samples (*Figure 8*)

$$\tan \delta_p = (\omega a_T)^m \qquad (12)$$

where $m = s_2 - s_1 = -0.04$. This means that the decrease of 5 decades in reduced frequency leads to the increase in tan δ_p by a factor of 1.6 (from 1 to 1.6 for $M_n = 2630$, and from 1.2 to 1.9 for $M_n = 710$, *Figure 10*). Dynamic mechanical results of Durand *et al.*[6] obtained on a CG

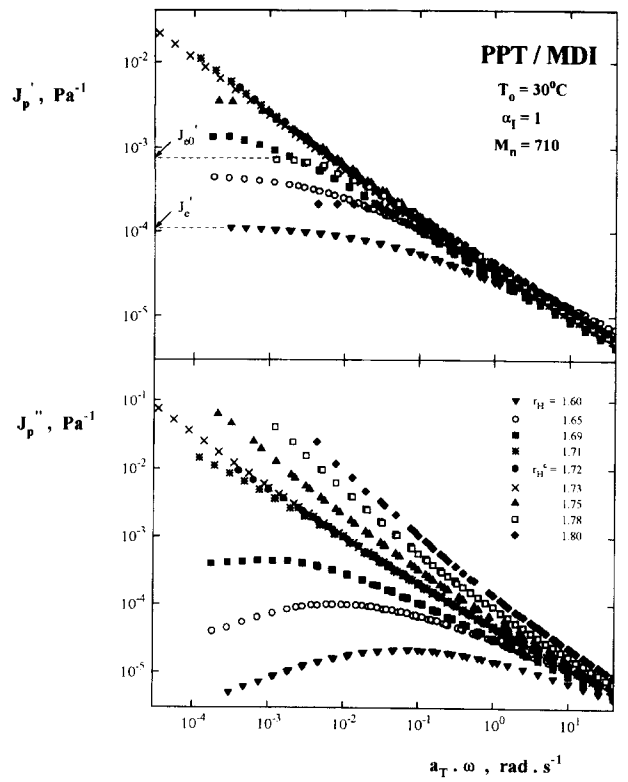

Figure 11 Dependence of the reduced storage and loss compliances, J'_p and J''_p, on the reduced frequency, ωa_T, for $T_0 = 30°C$ and triol LHT-240 for samples prepared at indicated r_H values

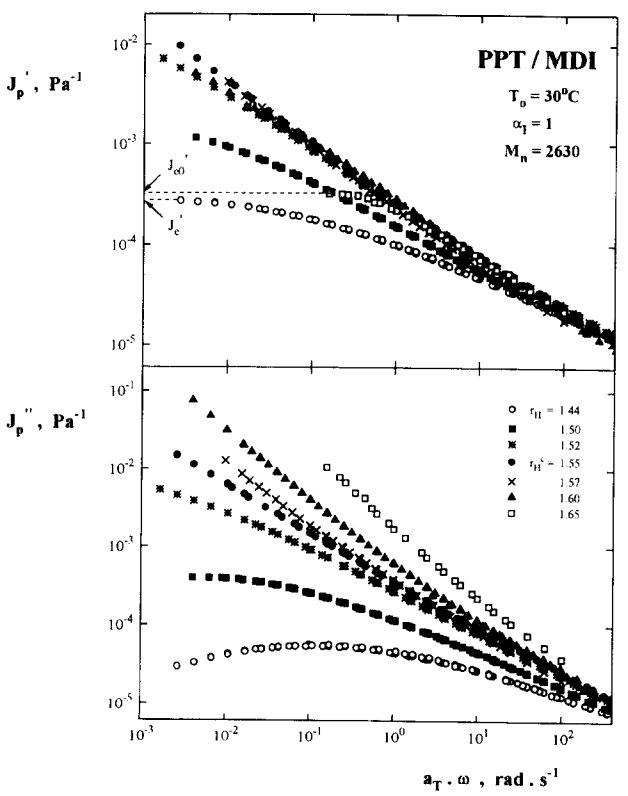

Figure 12 Dependence of the reduced storage and loss compliances, J'_p and J''_p, on the reduced frequency, ωa_T, for $T_0 = 30°C$ and triol LG-56 for samples prepared at indicated r_H values

polyurethane sample prepared from PPT and hexamethylene diisocyanate with an excess of OH groups also show an increase in the loss angle δ with decreasing frequency (see Figure 2 of ref. 6). We can thus conclude that the power-law behaviour with frequency-independent loss tangent is not exactly observed for chemically stable CG samples prepared by the CMR method.

An interesting behaviour can be seen in the frequency dependences of the superimposed storage and loss compliances, J'_p and J''_p, in the rubbery flow regions (*Figures 11* and *12*). For samples prepared at r_H^c, the linear dependences of $\log J'_p$ and $\log J''_p$ on $\log \omega a_T$ can be seen and the slopes s'_1 and s'_2 found for the storage [$s'_1 = -0.61$ (LHT-240) and -0.56 (LG-56)] and the loss [$s'_2 = -0.65$ (LHT-240) and -0.60 (LG-56)] compliance components differ. As in the case of the moduli, $s'_2 - s'_1 = -0.04$ for both samples. While the frequency dependences of J''_p and G''_p are qualitatively similar (in the flow region $J''_p \approx 1/G''_p$), distinct differences exist between the frequency dependences of J'_p and G'_p, and especially for samples with $r_H > r_H^c$.

From the phenomenological theory of linear viscoelastic behaviour the dynamic compliances are given by[16]

$$J'_p = J_g + \int_{-\infty}^{\infty} [L(\tau)/(1+\omega^2\tau^2)]\mathrm{d}(\ln\tau) \qquad (13)$$

$$J''_p = \int_{-\infty}^{\infty} [L(\tau)\omega\tau/(1+\omega^2\tau^2)]\mathrm{d}(\ln\tau) + 1/\omega\eta_0 \qquad (14)$$

where J_g is an instantaneous (glassy) compliance, η_0 is the steady-flow viscosity, $L(\tau)$ is the retardation spectrum and τ is the retardation time. From equation (13), setting $\omega = 0$, we have for the equilibrium compliance J_e in a viscoelastic solid or steady-state compliance J_{e0} in a viscoelastic liquid, the relations

$$J_e = \int_{-\infty}^{\infty} L(\tau)\mathrm{d}(\ln\tau) + J_g \qquad (15)$$

$$J_{e0} = \int_{-\infty}^{\infty} L(\tau)\mathrm{d}(\ln\tau) + J_g \qquad (16)$$

where J_g is generally negligible in comparison with the integrals.

For networks prepared with $r_H < r_H^c$, the limiting equilibrium compliances $J'_e = J_e$ (or the equilibrium moduli $G'_e = 1/J'_e$) can be extrapolated from the data for $\omega a_T \to 0$. On the other hand, for soluble samples with $r_H > r_H^c$ the limiting steady-state compliances $J'_{e0} = J_{e0} \neq 0$ can be found. The results presented in *Figures 11* and *12* correspond to these expectations. Both limiting compliances, J'_{e0} and J'_e, increase with decreasing deviation from the CG structure. The CG samples prepared at r_H^c show the highest J'_p values and linear dependences of $\log J'_p$ and $\log J''_p$ on $\log \omega a_T$ (i.e. extrapolation to $\omega a_T \to 0$ leads to infinite J'_{e0} and J'_e values). We believe that these features, especially the highest J'_p values at given ωa_T represent the limiting, critical dynamic mechanical behaviour of CG structures prepared by the CMR method.

Scanlan and Winter[4] pointed out the importance of the homogeneity of a CG sample. If a sample was inhomogeneous (due to nonisothermal curing) it was impossible to find tan δ independent of frequency. In our case the chemical reaction is rather slow. Hence, we believe that our CG samples after careful mixing

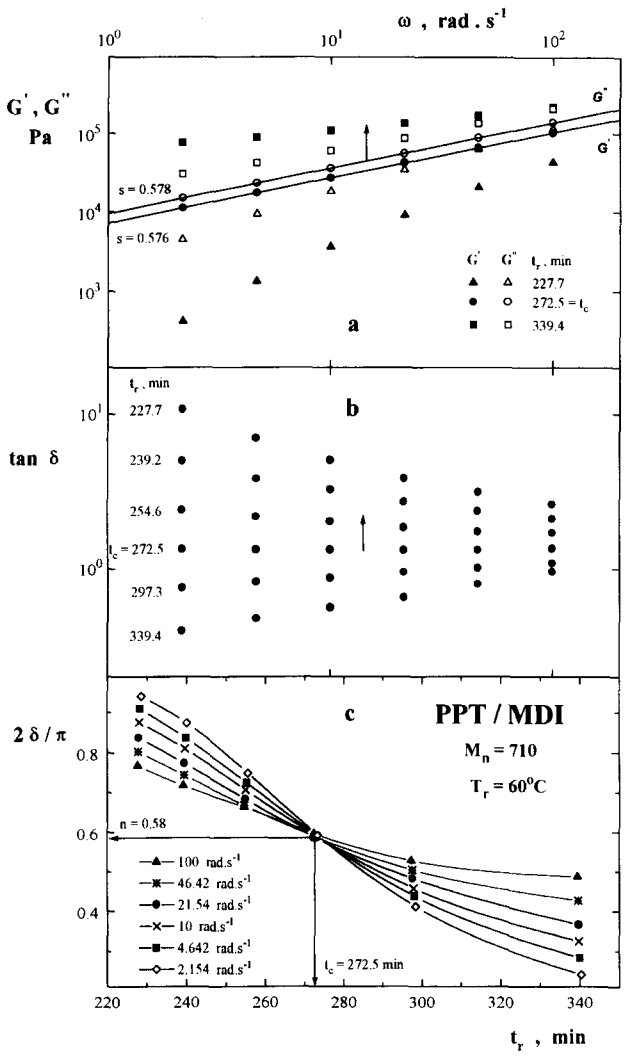

Figure 13 Dependence of dynamic moduli, G' and G'' (a), and of the loss tangent, tan δ (b), on frequency ω; (c) shows dependence of the ratio $2\delta/\pi$ on the reaction time, t_r. Samples prepared from triol LHT-240

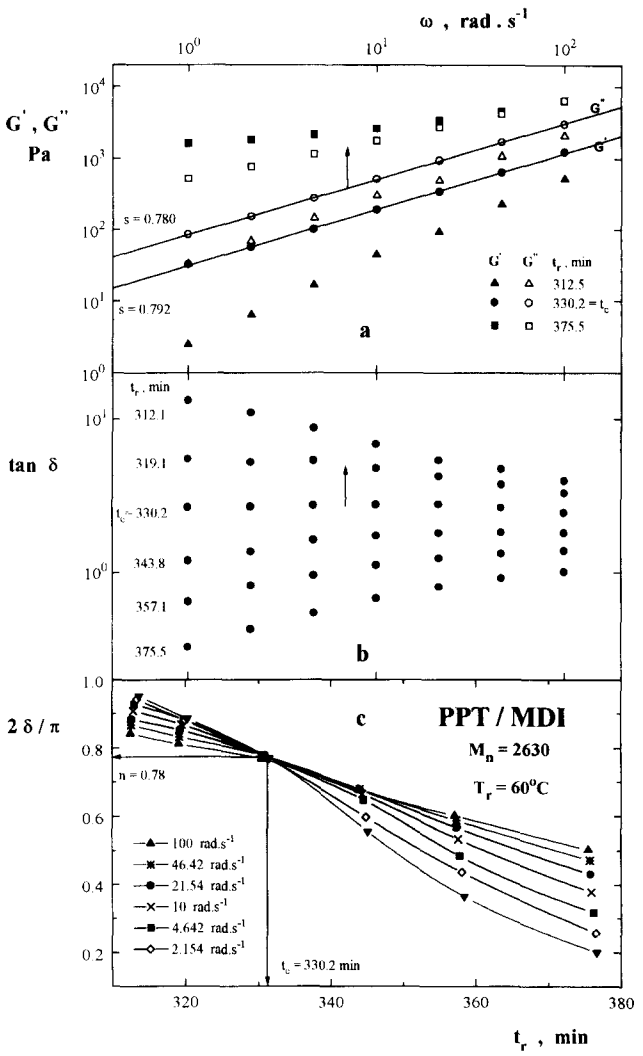

Figure 14 Dependence of dynamic moduli, G' and G'' (a), and of the loss tangent, tan δ (b), on frequency ω; (c) shows dependence of the ratio $2\delta/\pi$ on the reaction time, t_r. Samples prepared from triol LG-56

and good temperature control are homogeneous and the violation of power law behaviour is real. The same frequency dependence of tan δ_p observed in this rubbery and flow regions for samples with the values of r_H closest to the critical r_H^c value supports this conclusion.

As was mentioned in the Introduction, one may expect that frequency limits exist where power-law behaviour should be observed. The viscoelastic behaviour at very high frequencies (short times) is dominated by the local motion of monomeric units and parts of chains. This marks a short-time limit of the power-law region. From our results it follows that the end of the main transition region, characterized by the frequency of minima in the tan δ_p on ωa_T dependence, is this limit. On the other hand, a long-time limit of the power-law behaviour is neither expected nor observed.

Reacting systems at stoichiometric ratio $r_H = 1$. For comparison we have studied gelation of the stoichiometric systems ($r_H = 1$) for both triols at constant curing temperature $T_c = 60°C$. Generally, a stoichiometric mixture shows the earliest structure build-up and gel formation, along with the highest equilibrium G_e' modulus and gel fraction $w_g \to 1$ (the most perfect network is formed). Curing was followed at various frequencies of the dynamic measurements (one frequency scan took ~60 s) as a function of the reaction time, t_r. A typical evolution of the phase angle, δ, at six frequencies for both systems is shown in *Figures 13c* and *14c* for reaction times near the GP. The critical times occur at $t_c = 272.5$ min for LHT-240 and $t_c = 330.2$ min for LG-56. These relatively long gelation times correspond to slow reactions and one can expect very small changes of all the dynamic functions due to the changes in conversion during the short frequency sweeps lasting 60 s.

In *Figures 13b* and *14b* are shown interpolated values of the loss tangent tan δ (the interpolation gives only small corrections) as a function of frequency at six different reaction times t_r near the GP. As can be expected, tan δ decreases with ω in the liquid state ($t_r < t_c$) and increases with ω in the solid state ($t_r > t_c$). The relaxation exponents are calculated as $n = 0.58$ for LHT-240 and 0.78 for LG-56. The frequency dependences of the dynamic G' and G'' moduli shown in *Figures 13a* and *14a* demonstrate a power-law behaviour for the CG at t_c and the relaxation exponents

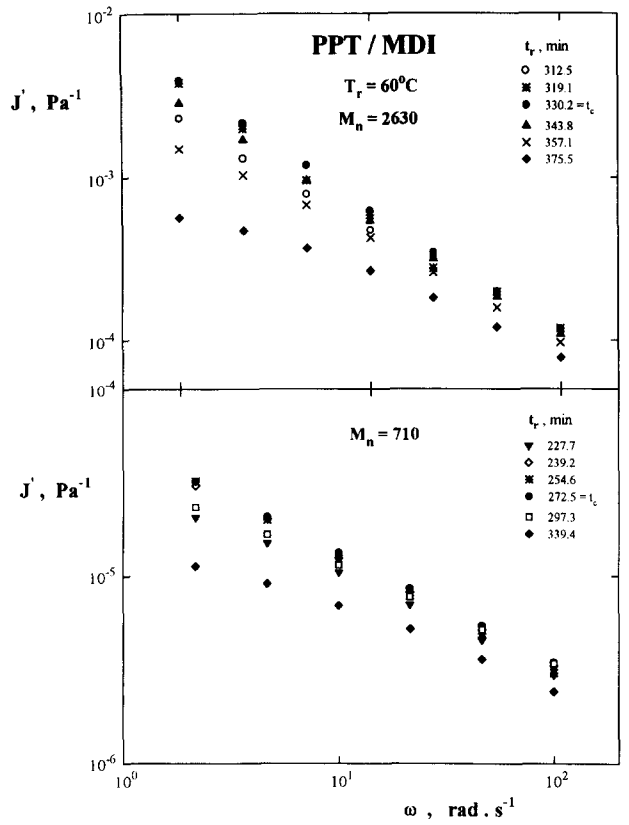

Figure 15 Dependence of the storage compliance, J', on frequency ω for both triols

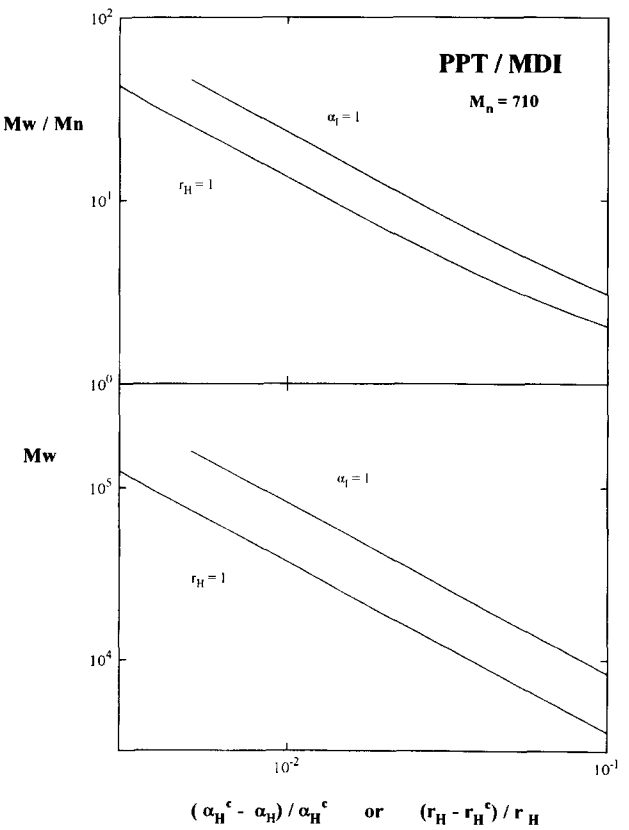

Figure 16 Dependence of weight-average molecular weight, M_w, and M_w/M_n ratio on the ratio $(\alpha_H^c - \alpha_H)/\alpha_H$ (for $r_H = 1$) or $(r_H - r_H^c)/r_H$ (for $\alpha_I = 1$) for triol LHT-240 calculated according to equations (17) and (18)

(slopes of log G' vs log ω plots) agree with those calculated from the phase angle. Before the GP the storage modulus G' rapidly decreases with decreasing ω after the GP it shows a rubbery plateau.

The frequency dependences of the storage compliances J' for both systems are shown in *Figure 15*. As in the case of stable samples, the highest J' values, the linear dependence of log J' on log ω and the infinite extrapolated values of J'_{e0} and J'_e are observed also for the CG structures prepared at t_c.

The storage and loss moduli, G' and G'', of CG samples were used for the calculation of the gel strength, S, using equation (2). Corresponding strength values calculated from *Figures 13a* and *14a* are $S = 7500$ *Pa* s^n for LHT-240 and $S = 60$ Pa s^n for LG-56. As was pointed out earlier[4], the CG rheological parameters are not universal because the values of the relaxation exponents n and of the gel strengths S depend on the molecular weight of the triol. In accord with previous results[4], a lower n value is connected with a higher S value and vice versa.

The power-law mechanical behaviour is due to the mechanical self-similarity which is a consequence of structural self-similarity developed during crosslinking reaction. The violation of the critical power-law rheological behaviour found for samples prepared at critical ratios r_H^c can be connected with the violation of structural self-similarity. If network formation takes place with an excess of hydroxyl groups up to full conversion of minority (isocyanate) groups, the structure of the system is very complex[10] (a network chain is composed of a backbone chain and many dangling chains). It can be expected that structure of the critical gel reached by a change in r_H will differ from that reached by a change in conversion. Any ring-free theory, regardless of the structure growth process, predicts for our case of network build-up the following relation for the number-average molecular weight M_n[7,14,19].

$$M_n = (n_H M_{n,H} + n_I M_{n,I}) \div [1 - (n_I f_{n,I}\alpha_I + n_H f_{n,H}\alpha_H)/2] \quad (17)$$

where n_I and n_H are the mole fractions of diisocyanate and triol in the reaction mixtures ($n_I + n_H = 1$), respectively. For the case of a random alternating stepwise addition of hydroxyl with isocyanate groups with independent reactivity the theory of branching processes gives the following equation for the increase in the weight-average molecular weight M_w[7,14,19].

$$M_w = [m_I M_{n,I}(D + F_{0I}F'_H) + m_H M_{n,I} F_{0H} + m_I M_{n,H} F_{0I} + m_H M_{n,H}(D + F_{0H}F'_I)]/D \quad (18)$$

where $m_I = n_I M_{n,I}/(n_I M_{n,I} + n_H M_{n,H})$, $m_H = 1 - m_I$, $F_{0I} = n_I f_{n,I}\alpha_I$, $F_{0H} = n_H f_{n,H}\alpha_H$, $F'_I = (f_{w,I} - 1)\alpha_I$, $F'_H = (f_{w,H} - 1)\alpha_H$ and $D = 1 - F'_H F'_I$. From the condition $M_w \to \infty$ [i.e. $D = 0$ in equation (18)], we get equation (3) valid for the gel point.

The calculated dependences [equations (17) and (18)] of the weight-average molecular weight M_w and M_w/M_n ratio on the critical conversion ratio, $(\alpha_H^c - \alpha_H)/\alpha_H^c$, or on the critical reactive groups ratio, $(r_H - r_H^c)/r_H$, for LTH-240 system are shown in *Figure 16*. As expected,

with decreasing critical reactive group and conversion ratios both the M_w and M_w/M_n values increase and the value of the critical exponent $\Delta = 1$ for the $M_w(M_w \sim [(\alpha_H^c - \alpha_H)/\alpha_H^c]^{-\Delta} \sim [(r_H - r_H^c)/r_H]^{-\Delta})$ and for the M_w/M_n ratio in the proximity of the gel point was proved. Lower M_w and M_w/M_n values found for the networks which were formed by changing the conversion in comparison with those formed by changing reactive group ratio are due to differences in the structure growth processes. The theory of branching processes thus predicts that the detailed CG structures reached by changes in conversion differ from those reached by changes in ratio of reactive groups, the latter being more polydisperse. This could be the reason for the observed differences in the CG dynamic mechanical behaviour of reacting and stable samples although the value of the critical exponent Δ did not change.

CONCLUSIONS

From the extraction and dynamic mechanical measurements carried out on the structurally stable (prepared by CMR method) and reacting (prepared by a change of conversion) polyurethane systems in the vicinity of the gel point the following conclusions can be made: (a) with non-reactive stable samples, prepared with an excess of hydroxyl groups to the full conversion of isocyanate groups, frequency–temperature superposition could be performed; the GP has no specific effect on the temperature dependence of the relaxation times (free-volume parameters of the WLF equation). (b) A small increase of the superimposed loss tangent, tan δ_p, with decreasing reduced frequency, ωa_T, found for stable GP samples at the lowest frequencies (tan $\delta_p \sim (\omega a_T)^m$, $m = -0.04$) shows that power-law behaviour at the GP is not exactly obeyed. (c) Reacting GP samples, obtained by curing at constant temperature and the stoichiometric ratio of reactive groups, exhibit a power-law rheological behaviour. The critical exponent n and the gel strength S depend on the molecular weight of the triol. (d) Both, structurally stable and reacting GP structures, show infinite values of the steady-state (J'_{e0}) and equilibrium (J'_e) storage compliances and the highest superimposed J'_p or J' values as functions of ωa_T or ω in the flow or rubbery regions. We believe that these features, especially the highest J'_p values at a given ωa_T represent the critical rheological behaviour at the GP.

ACKNOWLEDGEMENTS

Financial support of the Grant Agency of the Charles University (grant GAUK-169) and of the Grant Agency of the Academy of Sciences of the Czech Republic (grant A4050511) is gratefully acknowledged.

REFERENCES

1 Tung, CH-YM. and Dynes, P. J. J. *Appl. Polym. Sci.* 1982, **27**, 569
2 Chambon, F. and Winter, H. H. *Polym. Bull.* 1985, **13**, 499
3 Vilgis, T. A. and Winter, H. H. *Colloid Polym. Sci.* 1988, **266**, 494
4 Scanlan, J. C. and Winter, H. H. *Macromolecules* 1991, **24**, 47
5 Matějka, L. *Polym. Bull.* 1991, **26**, 109
6 Durand, D., Delsanti, M., Adam, M. and Luck, L. M. *Europhys. Lett.* 1987, **3**, 97
7 Stepto, R. F. T. In 'Biological and Synthetic Polymer Networks' (Ed. O. Kramer), Elsevier, London, 1988, p. 153
8 Stockmayer, W. H. *J. Polym. Sci.* 1952, **9**, 69; 1953, **11**, 424
9 Budinski-Simendić, J., Petrović, Z. S., Ilavský, M. and Dušek, K. *Polymer* 1993, **34**, 5157
10 Ilavský, M., Šomvársky, J., Bouchal, K. and Dušek, K. *Polym. Gels Networks* 1993, **1**, 159
11 Matějka, L. and Dušek, K. *Polym. Bull.* 1980, **3**, 489
12 Ilavský, M. and Dušek, K. *Polymer* 1983, **24**, 981
13 Ilavský, M. and Dušek, K. *Macromolecules* 1986, **19**, 2139
14 Dušek, K. in 'Telechelic Polymers: Synthesis and Applications' (Ed. E. Goethals), CRC Press, Boca Raton, 1989, p. 289
15 Flory, P. J. *Polymer* 1979, **20**, 1317
16 Ferry, J. D. 'Viscoelastic Properties of Polymers', 3rd Edn, Wiley, New York, 1980
17 Ilavský, M., Hasa, J. and Havlíček, I. *J. Polym. Sci. A-2*, 1972, **10**, 1775
18 Ilavský, M., Zelenka, J., Špaček, V. and Dušek, K. *Polym. Networks Blends* 1992, **2**, 95
19 Macosko, C. W. and Miller, D. R. *Macromolecules* 1976, **9**, 199
20 Dušek, K., Ilavský, M. and Luňák, S. *J. Polym. Sci., Polym. Symp.* 1975, **53**, 29
21 Gordon, M. and Malcolm, G. N. *Proc. R. Soc. London A* 1966, **A295**, 29